

Original Research Article

Isoconversional and Model-fitting approaches to Kinetic and Thermoanalytic study of Lanthanum oxalate: Nonlinear relationship between kinetic parameters.

ABSTRACT

The model-free and model-fitting kinetic approaches have been applied to data for nonisothermal and isothermal thermal decompositions of Lanthanum Oxalate. The popular model-fitting approach gives excellent fits for both isothermal and nonisothermal data but yields highly uncertain values of the Arrhenius parameters when applied to nonisothermal data using Coats-Redfern (CR) equation. These values cannot be meaningfully compared with the values derived from isothermal measurements, nor they can be used to reasonably predict the isothermal kinetics. On the other hand, the model-free approach represented by the isoconversional method such as Flynn-Wall-Ozawa (FWO) and Kissinger-Akahira-Sunose (KAS), yields similar dependencies of the activation energy on the extent of conversion for isothermal and nonisothermal experiments. The dependence derived from nonisothermal data permits reliable predictions of the isothermal kinetics. The use of the model-free approach is recommended as a trustworthy way of obtaining reliable and consistent kinetic information from both nonisothermal and isothermal data. The kinetic parameters although have a linear correlation between them, do not show isokinetic behaviour. Hence a better correlation between kinetic triplets was analysed using Nonlinear Compensation Law.

Keywords: Nonisothermal decomposition, Model free and model fitting methods, Kinetic parameters, Thermodynamic parameters, Isokinetic behaviour, Nonlinear compensation law

1. INTRODUCTION:

Kinetic analysis of thermal decomposition processes has been the subject interest for many investigators. The kinetics is intrinsically related with the decomposition mechanisms. The knowledge of the mechanism allows the postulation of kinetic equations or vice versa [1]. It is clear that the selection of correct model is a critical point in kinetic analysis. Knowing how a model can justify experimental data has been evaluated by many researchers [2-3]. There are different methods to study the kinetics of non-isothermal processes. These include statistical methods, Coats-Redfern (CR) method and iso-conversional model free methods. Activation energy, E_a values by using the

isoconversional model-free approaches such as modified Kissinger-Akahira-Sunose (KAS) and the Kissinger method, respectively were obtained[4] for the definite conversion intervals. A linear relationship has also been established between E and the change of the entropy ΔS^* for the formation of the activated complex from the reagents. These dependences are related to the assumption of identical kinetic mechanisms of thermal degradation of the composites studied [5].

For reactions with mixed mechanism, the CR method shows nonlinear trends and the reaction models and kinetic parameters cannot be extracted from CR curves and the approach is generally unsuitable for determination of kinetic parameters[6]. In non-isothermal kinetics, the use of the traditional methodology results in highly uncertain values of Arrhenius parameters that cannot be compared meaningfully with isothermal values hence the average results of non-isothermal experiments may be compared with isothermal analysis [7]. An alternative model-free methodology is based on the iso-conversional method. The use of this model-free approach in both isothermal and non-isothermal kinetics helps to avoid the problems that originate from the ambiguous evaluation of the reaction model. The model-free methodology allows the dependence of the activation energy on the extent of conversion to be determined. This in turn, permits reliable reaction rate predictions to be made and mechanistic conclusions to be drawn [8]. Therefore it is not really possible to determine the correct activation energy from a single non-isothermal curve. On the other hand, when a set of curves are recorded under different heating schedules are used, the correct kinetic parameters can be clearly discerned [9]. Experimental results showed that values of kinetic parameters from both model free and model fit methods are in good agreement and can be successfully used to understand the degradation mechanism of solid-state reaction [10].

The present work apply both model-fitting integral and model-free isoconversional methods to have significant and appreciable picture about the decomposition mechanism of Lanthanum Oxalate Decahydrate. The degree of reliability of parameters obtained from both the techniques are also studied. The kinetic parameters which generally fit to linear kinetic compensation law[11] have been revisited for better correlation from their nonlinearity and the authenticity of the kinetic data was tested by fitting into nonlinear compensation law so as to obtain true values.

2. MATERIAL AND METHODS:

Lanthanum Oxalate Decahydrate, was prepared as per our earlier work[12], using high purity AR grade $\text{La}(\text{NO}_3)_3$ and Ammonium Oxalate solution. The later was added drop wise with stirring for 30 min. White precipitate of Lanthanum Oxalate (LaOx) obtained was washed with distilled water and absolute alcohol, dried in vacuum oven at 70°C to constant weight. Lanthanum oxalate decahydrate powder obtained was characterised by FTIR, TEM, XRD etc. The sample was then heated at different temperatures ranging from room temperature to 900°C . Intermediates and final solid products were characterized by FTIR. Thermal TG/ DTA analysis of lanthanum oxalate were carried out at the heating rates of 3, 5 and 7°C min^{-1} up to 900°C in a dynamic atmosphere of air (20 ml/min), using SHEMATZU DTG 50 analyzer. The Isothermal decomposition of the same sample was also carried out at the temperatures i.e. 643, 653, and 663K.

3. RESULTS AND DISCUSSIONS:

3.1. FTIR analysis

The IR-spectrum of the solid phase LaOx-200 (Fig.1) bears a great deal of similarity to that of unheated $\text{La}_2(\text{C}_2\text{O}_4)_3 \cdot 10\text{H}_2\text{O}$ with absorption bands arising from oxalate anions ($1750\text{--}640\text{ cm}^{-1}$) and water of hydration ($3440, 1640\text{ cm}^{-1}$). The solid phase LaOx-300 IR-spectrum shows that the $\text{C}_2\text{O}_4^{2-}$ species are weakened and absorptions at 2350 cm^{-1} and between 1800 and 400 cm^{-1} , which is similar in shape and position to characteristic absorptions of CO_3^{2-} . Upon further heating the IR-spectrum of LaOx-400 lacks absorption due to water of hydration, which are strong, broad absorption observed in the spectrum of both the parent, LaOx-200 and LaOx-300 between 1600 and 1750 cm^{-1} . The fundamental modes of vibration of the CO_3^{2-} species between 1800 and 400 cm^{-1} are weakened and different band structure begin to appear between 1600 and 1300 cm^{-1} which is similar in shape and position to characteristic absorptions of oxycarbonates. The IR-spectrum LaOx-550 displays strong absorptions between 1600 and 1300 cm^{-1} and also at 1060 and 870 cm^{-1} assignable to oxycarbonate species. The absorption appearing at $730\text{--}500\text{ cm}^{-1}$ are related to La-O vibrational lattice mode. The IR-spectrum of LaOx-800 , shows no detectable absorptions due to oxycarbonate

species. The absorptions below 700 cm^{-1} are related to lattice vibration modes of La_2O_3 . The weak bands around 1600 , 1500 and 1380 cm^{-1} are most probably due to surface contamination by carbonate and moisture since it is known that La_2O_3 is a basic oxide.

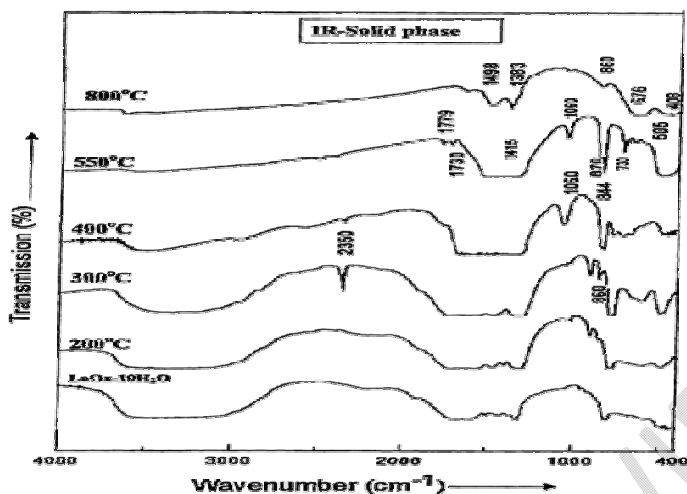


Fig.1: FTIR curves of LaOx at room temperature at temperatures 200, 300, 400, 550 & 800°C

3.2. TEM Analysis :

The general morphologies and microstructure of the sample was investigated by transmission electron microscopy (TEM), which illustrates that many needle-shaped particles are in the size range of 15-130 nm. The TEM images (Fig.2) reveal that most of the particles are uniform in size.

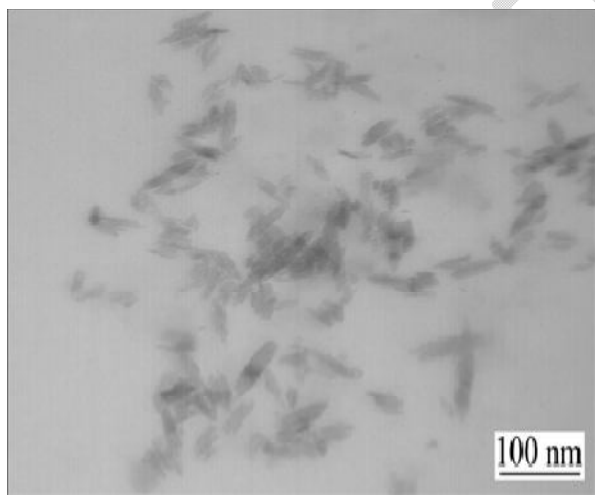


Fig.2: TEM image of $\text{La}_2(\text{C}_2\text{O}_4)_3 \cdot 10\text{H}_2\text{O}$

3.3. Thermal Analysis with X-ray diffraction:

The non-isothermal decomposition of lanthanum oxalate decahydrate $\text{La}_2(\text{C}_2\text{O}_4)_3 \cdot 10\text{H}_2\text{O}$ is investigated (Fig. 4) using rising temperature technique at 10 min^{-1} till $900\text{ }^\circ\text{C}$ in air. Intermediates and final solid products were characterized by X-ray diffraction (XRD) and FTIR-spectroscopy, the results show that $\text{La}_2(\text{C}_2\text{O}_4)_3 \cdot 10\text{H}_2\text{O}$ dehydrates decomposed in stepwise at $86\text{--}360\text{ }^\circ\text{C}$. The intermediates, $\text{La}_2(\text{C}_2\text{O}_4)_3$, $\text{La}_2\text{O}(\text{CO}_3)_2$ and $\text{La}_2\text{O}_2\text{CO}_3$, were formed at 400 , 425 and $470\text{ }^\circ\text{C}$, respectively. The final product La_2O_3 obtained at $800\text{ }^\circ\text{C}$ [13].

The corresponding XRD pattern (Fig. 3) of LaOx-200 indicates that the products are amorphous and so water of hydration is very important for the coherency of LaOx crystal.

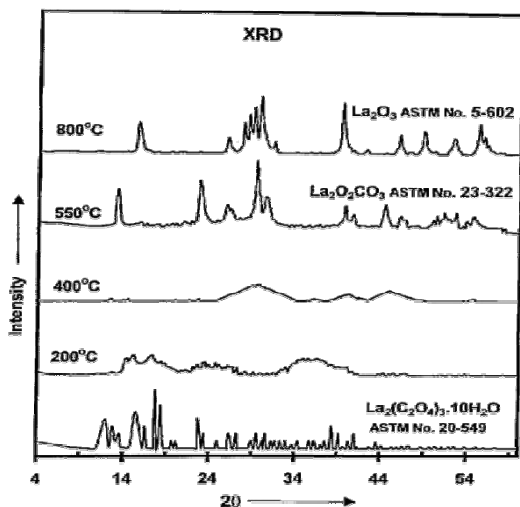


Fig. 3 : X-Ray diffraction patterns of decomposition products of lanthanum oxalate obtained at different temperatures

XRD pattern for LaOx-400 (Fig. 3), reveals that the $\text{La}_2(\text{CO}_3)_3$ product inferred from the TG and IR-data is amorphous. The event X accounts for the conversion of $\text{La}_2(\text{CO}_3)_3$ to $\text{La}_2\text{O}(\text{CO}_3)_2$ which converts immediately to $\text{La}_2\text{O}_2\text{CO}_3$ as follows:

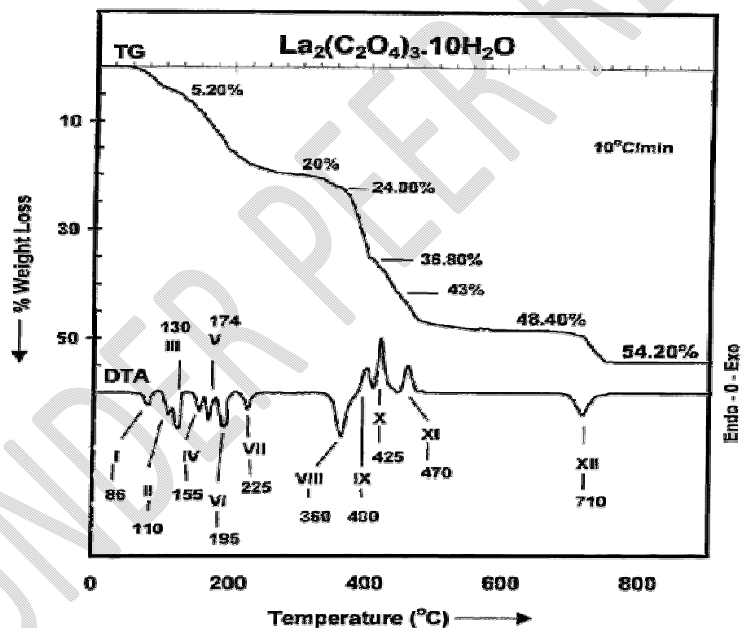
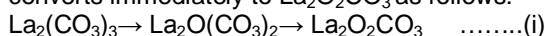


Fig.4: TG-DTA curve of Decomposition of Lanthanum Oxalate decahydrate heated up to 900°C

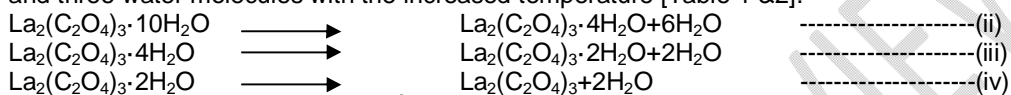
Events IX, X and XI must have overlapped between 420 and 550 °C. The IR-spectrum (Fig.1) and XRD patterns (Fig.3) support the above reaction. The corresponding XRD pattern for LaOx-550 shows the pattern for crystalline $\text{La}_2\text{O}_2\text{CO}_3$. In support of FTIR, the XRD pattern of LaOx-800 detect a crystalline phase of La_2O_3

Table-1: Thermal processes, temperature (°C), composition proposed in each process for $\text{LaOx} \cdot 10\text{H}_2\text{O}$

Process	Temperature(°C)	Composition
I	86	$\text{La}_2(\text{C}_2\text{O}_4)_3 \cdot 9\text{H}_2\text{O}$

II	110	$\text{La}_2(\text{C}_2\text{O}_4)_3 \cdot 8\text{H}_2\text{O}$
III	130	$\text{La}_2(\text{C}_2\text{O}_4)_3 \cdot 7\text{H}_2\text{O}$
IV	155	$\text{La}_2(\text{C}_2\text{O}_4)_3 \cdot 6\text{H}_2\text{O}$
V	174	$\text{La}_2(\text{C}_2\text{O}_4)_3 \cdot 5\text{H}_2\text{O}$
VI	195	$\text{La}_2(\text{C}_2\text{O}_4)_3 \cdot 4\text{H}_2\text{O}$
VII	225	$\text{La}_2(\text{C}_2\text{O}_4)_3 \cdot 2\text{H}_2\text{O}$
VIII	360	$\text{La}_2(\text{C}_2\text{O}_4)_3$
IX	400	$\text{La}_2(\text{CO}_3)_3$
X	425	$\text{La}_2\text{O}(\text{CO}_3)_2$
XI	470	$\text{La}_2\text{O}_2\text{CO}_3$
XII	710	La_2O_3

At the first stage the experimental mass loss (14.5%) is very close to the theoretical mass loss (14.9%), which could be attributed to the evolution of six water molecules. The second and third stages with a mass loss of about 4.9% and 5.03% respectively, can be assigned to the loss of two and three water molecules with the increased temperature [Table 1 & 2].



The fourth stage begins at 372.4 °C involving decomposition of $\text{La}_2(\text{C}_2\text{O}_4)_3$ to $\text{La}_2\text{O}_2(\text{CO}_3)$, a dioxy monocarbonate[12].

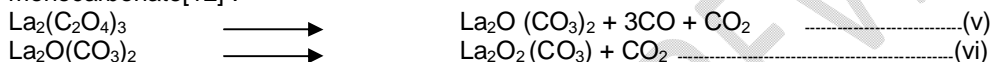
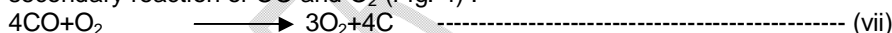


Table 2: Thermal decomposition data of $\text{La}_2(\text{C}_2\text{O}_4)_3 \cdot 10\text{H}_2\text{O}$

Temperature Range/°C	Mass change (%)		Solid residue
	Theoretical	Experimental	
40–226.2	14.9	14.5	Hexahydrate
226.2–295.2	4.99	4.9	Dihydrate
295.2–372.4	4.99	5.03	Anhydrous oxalate
372.4–600	23.8	27.2	$\text{La}_2\text{O}_2\text{CO}_3$
600–745.6	6.09	6.5	La_2O_3

Although the decomposition of oxalate is endothermic, the exotherms appear in DTA is due to secondary reaction of CO and O_2 (Fig. 4).



3.4. Kinetic Analysis :

For determination of Kinetic parameters, the TG curves are obtained at heating rates of 3, 5, and 7 °C min⁻¹ (Fig.5), show that the sample degraded between 370 °C and 550 °C. The maximum decomposition temperature, T_m and inception temperature T_0 increase with rate of heating. Furthermore, the area under the decomposition peak increased with increasing heating rate (Fig. 6).

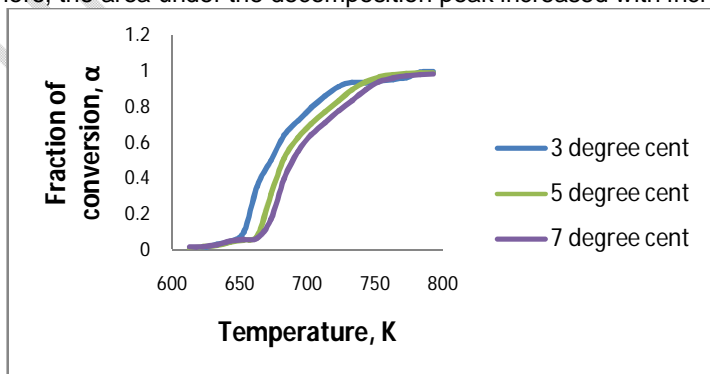


Fig.5 : Thermogravimetric curves for decomposition of lanthanum oxalate at different rate of heating

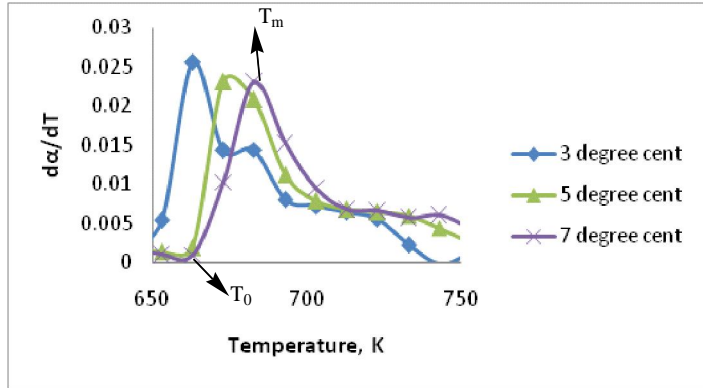


Fig.6: Derivative curves of lanthanum oxalate decomposition at different rates of heating

Isothermal decomposition curves for the lanthanum oxalate at three different temperatures also exhibit similar behaviour as in case of non-isothermal study and the “conversion-time” curve i.e. ‘α-t’, plot show upward shift with time, at higher temperatures (Fig.7).

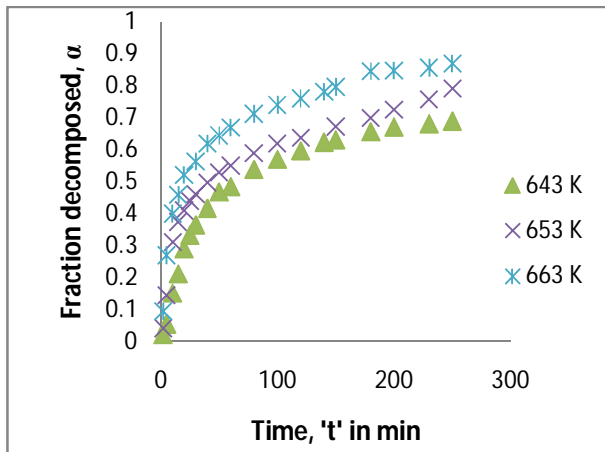


Fig.7: Conversion- time curve for isothermal decomposition of lanthanum oxalate

3.4.1. Nonisothermal method:

Kinetic parameters were obtained by both model-fitting Coat Redfern (CR) and iso-conversional model free (FWO & KAS) methods[15]. The Arrhenius parameters E and log A are obtained in the temperature region 380-480°C i.e. 653-753K (steps VIII- XI), for the best fit F3 mechanism model functions, $g(\alpha)$, and correlated by the compensation law[16]. The slopes and intercepts of the graphs $1/T$ vs. $\log [g(\alpha)/T^2]$ are obtained (Fig.8) at three different rates of heating using CR equation:

$$\log [g(\alpha)/T^2] = \log [AR/\beta E] - E/2.303RT \quad \dots\dots\dots(3).$$

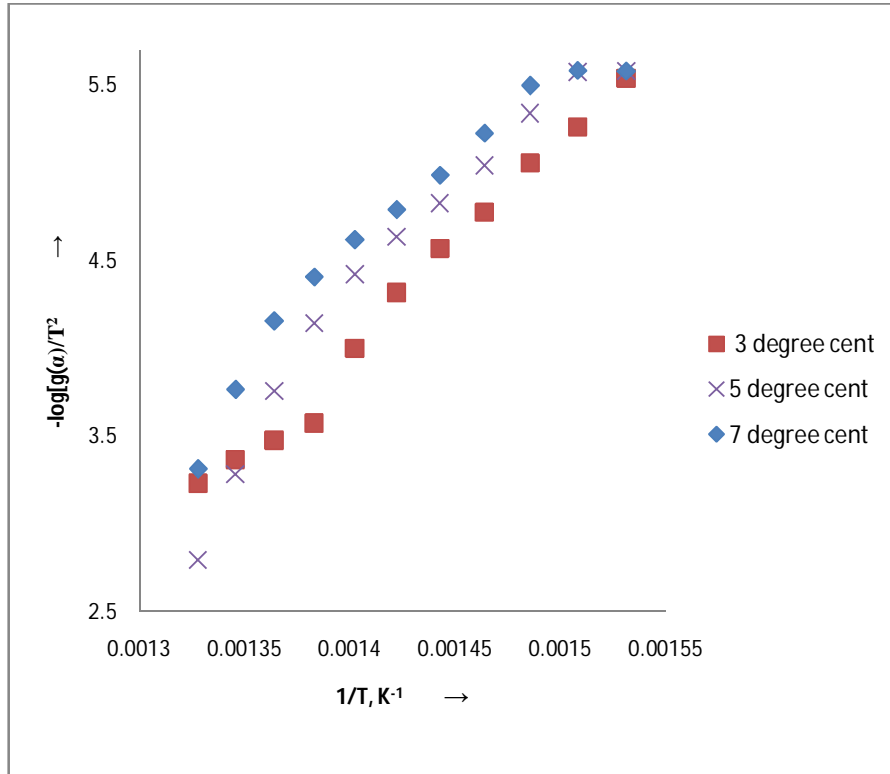


Fig.8: Variation of $-\log[g(\alpha)/T^2]$ with $1/T$ at different rate of heating

Iso-conversional analyses allow a complex processes to be detected by variation of E_a with α . The Kissinger–Akahira–Sunose(KAS) method is used in the form

$$\ln(\beta/T_\alpha^2) = \ln(A_\alpha R)/(E_{a,\alpha}g(\alpha)) - E_{a,\alpha}/R T_\alpha \quad (4)$$

Thus, for different values of α , $\ln(\beta/T_\alpha^2)$ and $1/T_\alpha$, were obtained from thermal curves at different heating rates, and straight lines are obtained for each ' α ' (Fig.9).The apparent activation energies, E and pre-exponential factors, $\log A$ are evaluated from the slopes and intercepts respectively.

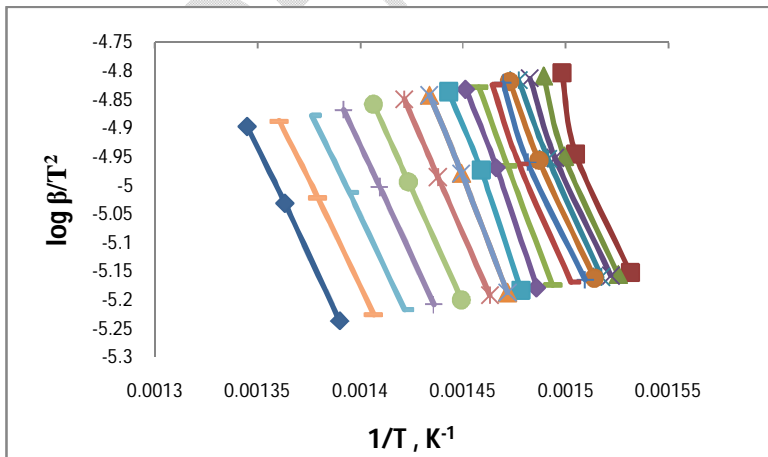


Fig 9: $\ln(\beta/T_\alpha^2)$ vs $1/T_\alpha$ plots

Similarly the Flynn–Wall–Ozawa (FWO) method is used in the form [17]

$$\ln \beta = \ln (A_{\alpha} E_{\alpha, \alpha} / (Rg(\alpha)) - 5.331 - 1.052 E_{\alpha, \alpha} / (RT_{\alpha}) \text{ -----(5)}$$

A graph between $\ln \beta$ and $1/T_{\alpha}$, are plotted for different α 's (Fig.10) which allow us to evaluate the E and $\log A$. The average values are calculated for comparison (Table-3).

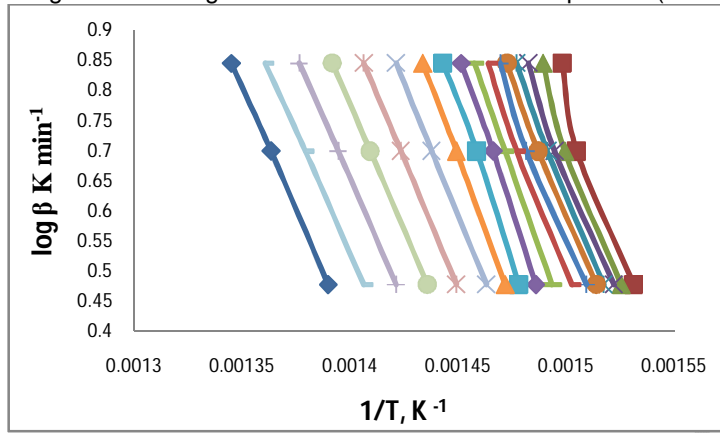


Fig.10 : $\log \beta$ — $1/T$ plots for E of the first endothermic peak by FWO method

3.4.2. Isothermal method:

Isothermal study in the temperature region 643-663K allow the calculation of kinetic parameters by correlating mechanism model function, $g(\alpha)$ with time ,t(Fig.11).The plot is a straight line with rate constant, k calculated from the slope using the equation:
 $g(\alpha)= kt + c$(1)

The rate, k was obtained at three different isothermal temperatures and presented [Table 4].The kinetic parameters E and A are obtained from slope and intercepts respectively, from the plot of $\ln k$ vs $1/T$ (Fig.12) using the Arrhenius equation ;
 $\ln k= \ln A - E/RT$ (2)

The isothermal and non-isothermal kinetic parameters are compared and presented in Table 3.

Table 3: Kinetic and Thermodynamic parameters of $La_2(C_2O_4)_3$ decomposition, by various methods

	$\beta, (^{\circ}Cmin^{-1})$	$E, (kJmol^{-1})$	$\log A, (min^{-1})$	$\Delta H^*, (kJmol^{-1})$	$\Delta S^* (Jmol^{-1}K^{-1})$	$\Delta G^* (kJmol^{-1})$
Coat-Redfern Method	3	230.33	16.00	224.76	46.34	193.71
	5	255.50	17.94	249.92	83.46	194.01
	7	209.26	14.32	203.69	14.26	194.13
	Average	231.70	16.09	226.12	48.02	193.95
Isoconversional Methods	FWO	167.98	11.05	162.41	-48.46	194.88
	KAS	165.26	10.06	159.69	-52.25	194.70
Isothermal Method		303.03	23.16	298.77	148.19	199.48

Table 4 :Rate constants obtained at different isothermal temperatures

k, sec^{-1}	T, K	$1/T, K^{-1}$	$-\log k$
0.038819	643	0.00155521	1.41096
0.069832	653	0.001531394	1.15595
0.215161	663	0.001508296	0.66724

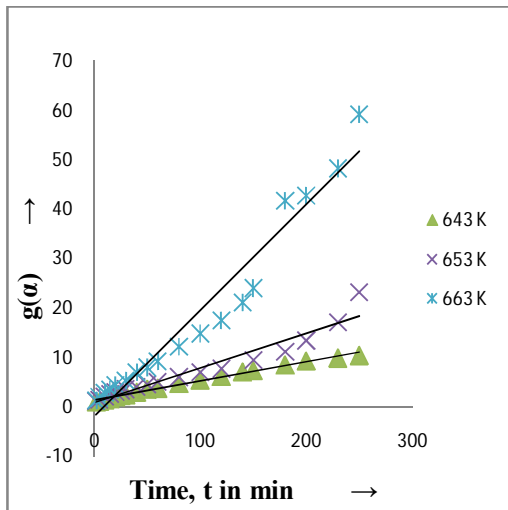


Fig.11: Variation of $g(\alpha)$ with time ,t at different temperatures

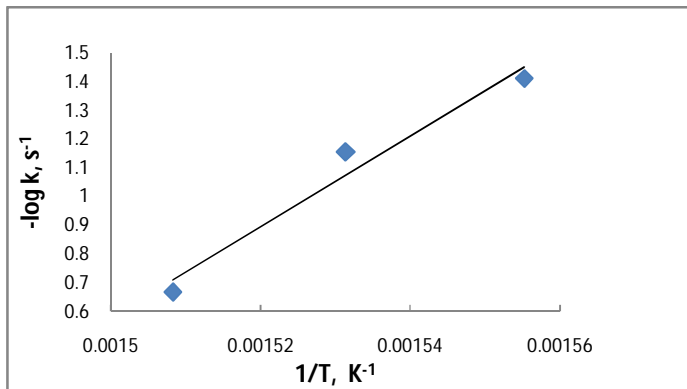


Fig.12 : Variation of T^{-1} with $-\log k$ during isothermal decomposition of lanthanum oxalate

The apparent activation energy for the degradation of lanthanum Oxalate is not same at all conversion, α (Fig. 13), indicates the existence of a complex multistep mechanism that occurs in the solid state. The kinetic and thermodynamic parameters for both model fitting and model free methods are presented [Table 3].

The values of apparent activation energy (E_a) calculated by model free (KAS and FWO) methods are in conformity with the reported activation energy in many studies i.e. 177.5 kJ/mol [18] and lower than values of E_a calculated by integral non- isothermal (Coat-Redfern) and isothermal methods . Thermodynamic parameters e.g. entropy of activation (ΔS^*), enthalpy of activation (ΔH^*) and Gibbs free energy (ΔG^*) were calculated using Equations (6)-(9).

$$A = (kT/h)e^{(\Delta S^*/R)} \quad \dots\dots\dots (6)$$

$$\Delta H^* = \Delta E - RT \quad \dots\dots\dots (7)$$

$$\Delta G^* = \Delta H^* - T\Delta S^* \quad \dots\dots\dots (8)$$

where h and k are Planck's constant and Boltzmann constant respectively.

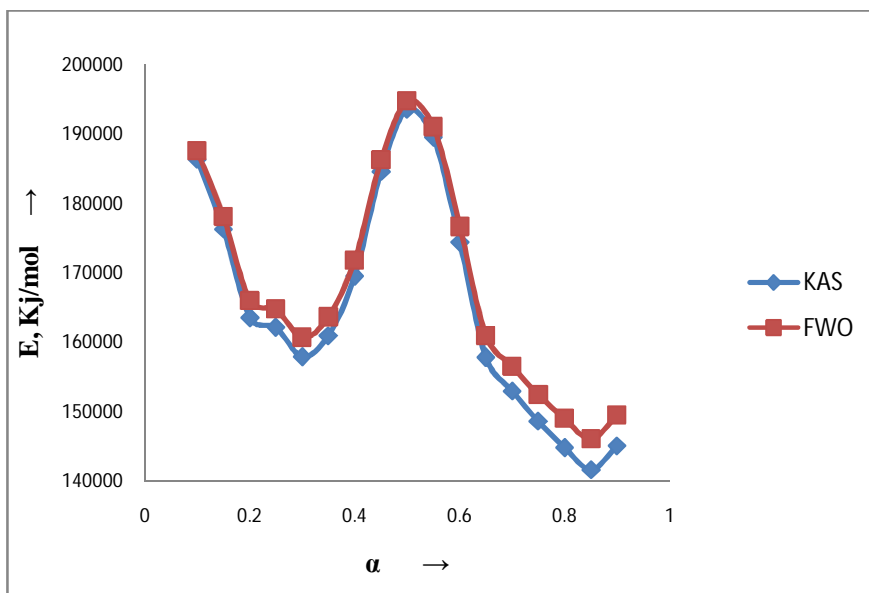


Fig. 13: Variation of activation energies, E with degree of conversion, α

It is observed that the entropy of activation increases with the increase of activation energy. The positive value of ΔG shows that the reaction involved in the decomposition of Lanthanum oxalate is not spontaneous. It is noted that the activation energy is nearly equal to enthalpy of activation, suggesting that Lanthanum oxalate is in condensed phase at 653-753K. The values of ΔS^* for isoconversional methods are negative, indicating that the corresponding activated complex has a higher degree of arrangement (lower entropy) than that in the initial state. The data on kinetic and thermodynamic parameters using various methods are presented in Table- 3.

In case of isothermal method the E has the highest value and this discrepancy may be due to the F3 mechanism which could be different in case of isothermal study. Moreover the rising temperature technique that uses CR equation with F3 model function also reported higher value of E. This may be attributed to the fact that, for $\alpha < 0.70$ in the chosen temperature range and the plot of $\log[g(\alpha)/T^2]$ versus $1/T$ is linear, indicating that the reaction is a single mechanism. However for extents of reaction $\alpha > 0.7$ the reaction has multi model mechanisms, for which the CR eqn. cannot be used showing a nonlinear trend (Fig.8). Therefore it is ascertained that kinetics of complex a reactions, where the reaction model changes with the extent of reaction, cannot be analysed with CR method with absolute correctness.

Further from isoconversional methods it is evident that E depends on α , demonstrating that the decomposition reaction process of the lanthanum oxalate is of complex kinetic mechanism [19]. Hence the kinetic parameters derived may be considered to be apparent and not true. The activation energies, E calculated by various methods are presented in bar diagram(Fig. 14)

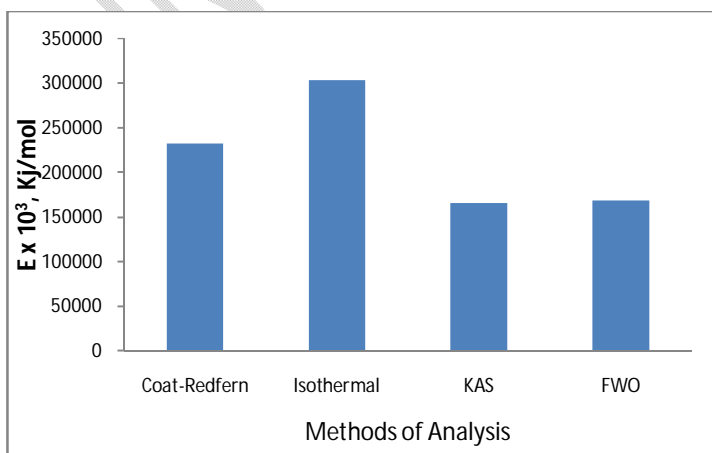


Fig. 14: variation of activation energies with methods of analysis

3.4.3. Kinetic compensation effect:

It is found that the variation in apparent activation energy, E is accompanied by a change $\ln A$. This phenomenon is often referred to as the Kinetic compensation effect (KCE), often coexistent with isokinetic point ($1/T_{iso}, \ln k_{iso}$). In such cases, the changes in pre-factor and apparent activation enthalpy display a linear dependency according to the Cremer-Constable relation[20].

$$\ln A = aE + b \quad \dots\dots\dots(9)$$

Where a and b are constant coefficients for a series of related rate process and are called compensation parameters. The rate constant, 'k' is temperature dependent, and is usually described well by Arrhenius relationship:

$$k = A e^{-E_a/RT} \quad \dots\dots\dots(10)$$

$$\ln A = \ln k + E/RT \quad \dots\dots\dots(11)$$

Although the experimental data showed that a plot of $\ln A$ vs E (Fig.15) and $\log k$ vs $1/T$ (Fig.16) different methods in the temperature range 653K-753K, are all linear, but fail to display a single point of concurrence i.e. isokinetic point ($1/T_{iso}, \log k_{iso}$). Hence the kinetic parameters exhibit a false compensation effect and are with their apparent values.

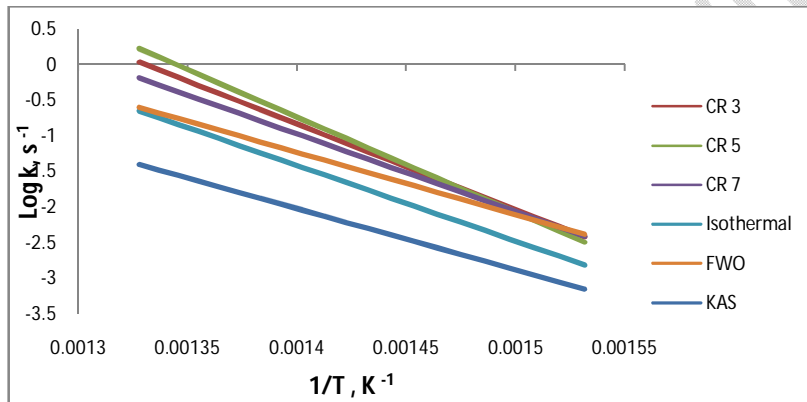


Fig.16 : Variation of $\log k$ with $1/T$ for different methods of analyses.

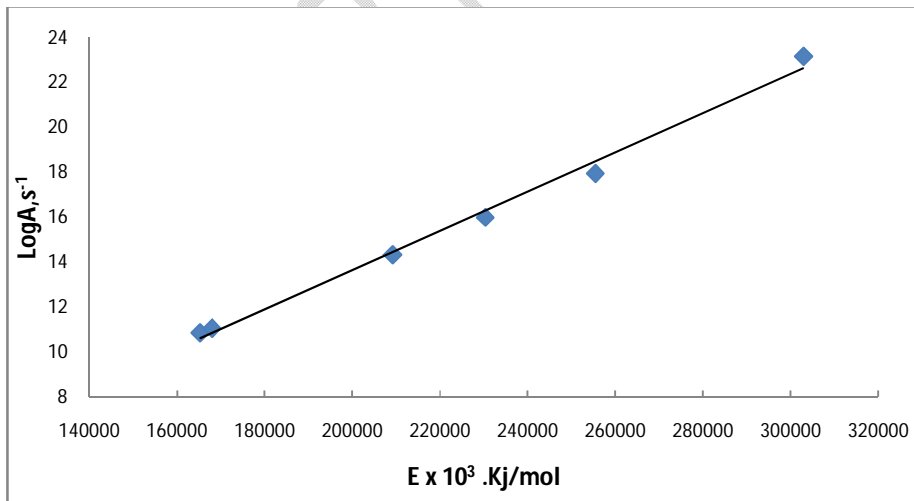


Fig.15 : Variation of $\log A$ with E and verification of Kinetic Compensation Effect

3.4.4. Non linear Compensation law and kinetic parameters:

The correlation derived between the kinetic parameter E and $\log A$ from TG curves can be described by means of Non linear compensation law[21] expressed as

$$\log A' = (RT_{0.1} \ln 10)^{-1} E + \log(\beta E/T_{0.1}^2) - 1.85 \dots\dots\dots(12)$$

Where $T_{0.1}$ is the temperature at which the conversion attains a degree of 0.1 ($\alpha = 0.1$). The equation is not a linear and therefore it is not an iso-kinetic relation. However the relationship becomes iso-kinetic provided $\log(\beta E/T_{0.1}^2)$ is constant, which is not found in the present work. The true values of pre factor $\log A'$ is varies with rates of heating, β and presented along with $\log(\beta E/T_{0.1}^2)$ [Table-5] for both model fitting and model free methods of analyses.

Table-5: Corrected approximation for pre-exponential factors using nonlinear compensation law

	β	$\log(\beta E/T_{0.1}^2)$	$\log A', (s^{-1})$
CR	3	0.2096	16.572
	5	0.4614	18.692
	7	0.5169	15.04
FWO	3	0.0725	11.657
	5	0.2792	11.632
	7	0.4214	11.715
KAS	3	0.0655	11.433
	5	0.2721	11.411
	7	0.4144	11.495

4. CONCLUSION

It was found that the activation energy cannot be reliably determined by applying model-fitting methods of kinetic analysis to data obtained under non isothermal experimental conditions. Thus, the use of a set of curves recorded under different heating schedules is necessary, as recently recommended by the ICTAC Kinetics Committee [22]. It is also important to consider the nature of the reaction under study since only one step processes can be analyzed by this methodology. More complex or multiple step reactions require the use of isoconversional methods or the deconvolution of the individual steps. The kinetic parameters of lanthanum Oxalate decomposition to corresponding carbonate obeys kinetic compensation behaviour however the effect is a false compensation effect. A more correct description of the correlation between E and $\log A$ is given by non-linear compensation law which is a good approximation

COMPETING INTERESTS

There is not any potential conflicts of interest like employment, consultancies, honoraria, paid expert testimony, patent applications/registrations, and grants or other funding etc. There is no financial and personal relationships with other people or organizations that could inappropriately influence (bias) the work.

REFERENCES

- [1] J. Jach in "reactivity of solids" (Ed. J.H. De. Boer) Elsevier, Amsterdam, 1961 pp. 334
- [2] J.Jach; The thermal decomposition of NaBrO_3 part I-Unirradiated material, J. Phys, Chem solids 1963, 24, 63
- [3] A.K.Galway,in "Int.Rev.Sc."Inorg.chem.Series II.Butterworth, London 1975, 10,147
- [4] V.V.Boldyrev, Topochemistry of Thermal decomposition of solids, Thermochim.Acta,1986 100, 315

- [5] J. Physiak, and B.P. Wasia J. Therm. Anal, 1984, 29, 829
- [6] R. Ebrahimi-Kahrizsangi, M.H. Abbasi; Evaluation of reliability of Coats-Redfern method for Kinetic analysis of non-isothermal TGA. Trans. Nonferrous Met. Soc. China, 2008, 18, 217-221
- [7] Xia Yongjiang, Xue Huaqing, Wang Hongyan, Li Zhiping, Fang Chaohe; Kinetics of isothermal and non-isothermal pyrolysis of oil shale; Oil Shale, 2011, 28, 415-424
- [8] Sergey Vyazovkin and Charles A. Wight; Isothermal and non-isothermal kinetics of thermally stimulated reactions of solids; International Reviews in Physical Chemistry, 1998, 17, 407-433
- [9] Pedro E Sánchez-Jiménez, Luis A Pérez-Maqueda, Antonio Perejón and José M Criado Clarifications regarding the use of model-fitting methods of kinetic analysis for determining the activation energy from a single non-isothermal curve; Chemistry Central Journal 2013, 7, 25 (Short Communication)
- [10] K. Slopiecka, P. Bartocci, F. Fantozzi; Thermogravimetric analysis and Kinetic study of poplar wood pyrolysis Third International Conference on Applied Energy 2011: 1687-1698
- [11] Z. Adonyi and G. Korosi; Experimental Study of Non-isothermal Kinetic equations and compensation effect; Thermochimica Acta, 1983, 60: 23-45
- [12] Nayak H, Pati S. K, Bhatta. D. Decomposition of γ -irradiated $\text{La}_2(\text{C}_2\text{O}_4)_3 + \text{CuO}$ mixture: A non-isothermal study; Radiation Effects and Defects in Solids, 2004, 159: 93-106.
- [13] Basma A.A. Balboul, A.M. El-Roudi, Ebthal Samir, A.G. Othman; Non-isothermal studies of the decomposition course of lanthanum oxalate decahydrate, Thermochimica Acta, 2002 387: 109-114
- [14] P. Simon, Isoconversional methods-Fundamental, meaning and application; J. Therm. Anal. Calorim. 2004, 76: 123
- [15] S. Vyazovkin, C.A. Wight, Model free and model fitting approaches to Kinetic analysis of isothermal and nonisothermal data; Thermochim. Acta, 1999, 340/341: 53
- [16] B. Jankovic; Kinetic analysis of the nonisothermal decomposition of potassium metabisulfite using the model-fitting and isoconversional (model-free) methods Chemical Engineering Journal, 2008, 139: 128-135
- [17] ZHAN Guang, YU Jun-xia, XU Zhi-gao, ZHOU Fang, CHIRu-an; Kinetics of thermal decomposition of lanthanum oxalate hydrate; Trans. Nonferrous Met. Soc. China, 2012, 22: 925-934
- [18] Obaid A Y, Alyoubi A O, Samarkandy A A, Al-Thabaiti S A, Al-Juaid S S, Ei-Bellahi A A, Ei-Deifallah H M.; Kinetics of thermal decomposition of copper(II) acetate monohydrate. Therm Anal Calorim, 2000, 61(3): 985-994.
- [19] Bond, G. C.; Keane, M. A.; Kral, H.; Lercher, J. A. Catal. Rev.-Sci. Eng. 2000, 42(3): 319-327
- [20] J. Zsako, Kinetic analysis of Thermogravimetric data xxxi. Derivation of non-linear kinetic compensation law, Journal of Thermal analysis, 1998, 54: 921-929
- [21] Vyazovkin S, Burnham AK, Criado JM, Perez-Maqueda LA, Popescu C, Sbirrazzuoli N: ICTAC Kinetics Committee recommendations for performing kinetic computations on thermal analysis data. Thermochim Acta, 2011, 520: 1-19.